

BAP1 controls mesenchymal stem cell migration by inhibiting the ERK signaling pathway

Seobin Kim^{1,2}, Eun-Woo Lee^{3,4}, Doo-Byoung Oh^{1,2,*} & Jinho Seo^{1,2,*}

¹Aging Convergence Research Center, Korea Research Institute of Bioscience and Biotechnology (KRIBB), Daejeon 34141, ²Department of Biosystems and Bioengineering, University of Science and Technology (UST), Daejeon 34113, ³Metabolic Disease Research Center, KRIBB, Daejeon 34141, ⁴Department of Functional Genomics, UST, Daejeon 34113, Korea

Due to their stem-like characteristics and immunosuppressive properties, Mesenchymal stem cells (MSCs) offer remarkable potential in regenerative medicine. Much effort has been devoted to enhancing the efficacy of MSC therapy by enhancing MSC migration. In this study, we identified deubiquitinase BRCA1-associated protein 1 (BAP1) as an inhibitor of MSC migration. Using deubiquitinase siRNA library screening based on an *in vitro* wound healing assay, we found that silencing BAP1 significantly augmented MSC migration. Conversely, BAP1 over-expression reduced the migration and invasion capabilities of MSCs. BAP1 depletion in MSCs upregulates ERK phosphorylation, thereby increasing the expression of the migration factor, osteopontin. Further examination revealed that BAP1 interacts with phosphorylated ERK1/2, deubiquitinating their ubiquitins, and thus attenuating the ERK signaling pathway. Overall, our study highlights the critical role of BAP1 in regulating MSC migration through its deubiquitinase activity, and suggests a novel approach to improve the therapeutic potential of MSCs in regenerative medicine. [BMB Reports 2024; 57(5): 250-255]

INTRODUCTION

Mesenchymal stem cells (MSCs) derived from mesodermal lineage tissues can self-renew and differentiate into various cell types that include osteoblasts, adipocytes, and chondrocytes (1). Furthermore, their ability to secrete cytokines and growth factors provides them with unique immunomodulatory and immunosuppressive properties, such as increased generation of regulatory T-cells and M2 macrophages, while suppressing

B- and T-cell proliferation and monocyte maturation (2-5). These properties have led to hundreds of clinical trials being conducted to treat a wide range of diseases, including neurodegenerative, metabolic, and inflammatory diseases, as well as tumors (6, 7). Furthermore, adoptively transferred MSCs can migrate to the target injury sites to regenerate damaged tissues (7). Migration is regulated by various chemokine receptors, adhesion molecules, and molecular signaling pathways. Therefore, many studies have attempted to improve the migration ability of MSCs for clinical benefits (8, 9).

Ubiquitination and deubiquitination are reversible post-translational modification (PTM) processes that modulate numerous cellular protein functions. This modification can induce proteasomal or lysosomal degradation, change enzymatic activity, or modify cellular signaling pathways (10). Deubiquitination, the removal of attached ubiquitin(s) by a deubiquitinase, can reverse the effects of ubiquitination. To date, one hundred deubiquitinases have been identified, and classified into seven superfamilies (11). Most deubiquitinases utilize a catalytic cysteine residue in conjunction with histidine in the deubiquitinase domain to hydrolyze the ubiquitin linkage (11). BRCA1-associated protein 1 (BAP1) was previously known as a tumor suppressor, and also identified as a deubiquitinase containing the ubiquitin C-terminal hydrolase (UCH) domain in its N-terminal region (12). Additionally, BAP1 modulates transcription, DNA repair, and replication by regulating chromatin remodeling via histone H2AK119 deubiquitination (12). Although histone H2AK119 deubiquitination is known as the principal target of BAP1, recent studies have reported several non-histone targets, including IP3R3, HCF-1, KLF5, INO80, DNA methyltransferase 1 (DNMT1), nuclear receptor corepressor-1 (NCOR1), and peroxisome proliferator-activated receptor-gamma coactivator 1-alpha (PGC1 α) (13-18).

Although ubiquitination-deubiquitination has been highlighted in various cellular events, its role in MSC migration has yet to be reported, and remains unclear. In this study, we identified BAP1 as a negative regulator of MSC migration using wound healing-based deubiquitinase siRNA library screening. The deubiquitinase activity of BAP1 is required to inhibit the ERK signaling pathway and MSC migration, suggesting that BAP1 suppresses MSC migration by deubiquitinating ERK ubiquitin.

*Corresponding authors. Doo-Byoung Oh, Tel: +82-42-860-4457; Fax: +82-42-879-8299; E-mail: dboh@kribb.re.kr; Jinho Seo, Tel: +82-42-879-8296; Fax: +82-42-879-8299; E-mail: sjh0130@kribb.re.kr

<https://doi.org/10.5483/BMBRep.2023-0174>

Received 14 September 2023, Revised 19 October 2023,
Accepted 9 November 2023, Published online 21 February 2024

Keywords: BAP1, Cell migration, Deubiquitination, ERK, Mesenchymal stem cell

RESULTS

BAP1 deficiency enhances MSC migration

To identify the deubiquitinases that regulate MSC motility, we performed primary screening based on an *in vitro* wound healing assay using 99 deubiquitinase siRNAs (Supplementary Fig. 1 of the Supplementary Information [SI]). This screening identified 13 potential candidates comprising five inhibitors and eight activators (Fig. 1A). To narrow down the deubiquitinase candidates, we performed triplicate analyses, and selected BAP1 as the deubiquitinase that exerted the most significant impact on MSC motility (Fig. 1B, C). Compared to siNon-transfected MSCs, BAP1 depletion in MSCs using siRNA transfection increased the wound closure rate by up to 50% (Fig. 1B, D, E). Transwell migration and invasion assays were performed to investigate the effects of BAP1 depletion on MSC migration. MSCs depleted of BAP1 displayed dramatic increases in Transwell migration and invasion (Fig. 1F, G).

We used the Human Protein Atlas portal (www.proteinatlas.org), a freely available interactive resource, to examine the BAP1 mRNA expression patterns across various tissues. Compared to the other tissues, blood cells, which exhibit high motility, showed markedly lower levels of BAP1 expression (Supplementary Fig. 2 of the SI). Remarkably, bone marrow and adipose tissue, which are the primary sources of MSCs, display relatively high levels of BAP1 expression. These observations suggest that BAP1 expression is correlated with cell motility, reinforcing our finding that BAP1-depleted MSCs showed enhanced migration.

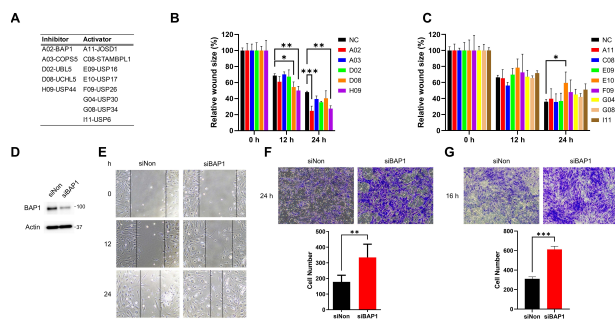


Fig. 1. BAP1 depletion promotes MSC migration. (A) A table of the siRNA screening results. (B-G) The MSCs were transfected with 20 nM siNon or deubiquitinase siRNAs. The cells were scratched, visualized by a bright field microscope (E), and further analyzed using Image J software (B, C). Data are presented as the mean \pm standard deviation (SD) from three independent experiments. Statistical analysis was performed using two-way ANOVA. Significances were computed by Tukey's honestly significant difference (HSD) (* $P < 0.05$, ** $P < 0.01$, and *** $P < 0.001$). (D) BAP1 protein levels were determined by immunoblotting. For the transwell migration (F) and invasion analysis (G), data are presented as the mean \pm SD from three independent experiments. Statistical analysis was performed using Student's *t*-test (** $P < 0.01$ and *** $P < 0.001$).

BAP1 overexpression reduces MSC migration

To further investigate whether BAP1 overexpression induced the opposite effect of BAP1 depletion on MSC migration, we performed wound healing, transwell migration, and invasion assays under BAP1 overexpression conditions. Given the inherent difficulty in transfecting MSCs, we used a CpG sequence-free plasmid-based microporation method (19). Following microporation with the pCGfd-GFP plasmid under optimized conditions, most of the MSCs exhibited GFP-positive signals (Fig. 2A). Subsequent immunoblot analysis of the MSCs transfected with the pCGfd-HA-BAP1 plasmid showed strong signals when probed with an anti-HA antibody (Fig. 2B). We analyzed the effects of BAP1 overexpression on MSC motility. BAP1 overexpression in the MSCs decreased the wound closure rate by up to 40% compared to the control MSCs (Fig. 2C, D). Transwell migration and invasion assays revealed that BAP1 overexpression inhibited MSC migration and invasion (Fig. 2E, F).

All the results obtained in both the BAP1 depletion and overexpression experiments indicate that BAP1 plays a crucial role in regulating MSC migration.

The deubiquitinase activity of BAP1 is essential for the regulation of MSC migration

BAP1 possesses a UCH domain with deubiquitinase activity in its N-terminal region (Supplementary Fig. 3A of the SI) (12). To explore whether the deubiquitinase activity of BAP1 is required for the regulation of MSC migration, we created a deubiquitinase-defective BAP1 C91S mutant (Supplementary Fig. 3A of the SI). Unlike the wild-type BAP1 expression, expression of

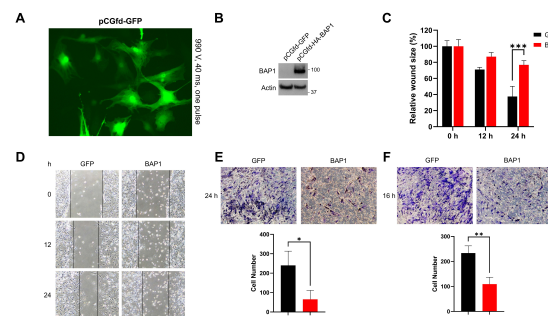


Fig. 2. BAP1 expression hinders MSC migration. (A) MSCs, 24 h post-pCGfd-GFP transfection, were visualized using a fluorescence microscope. (B) MSCs transfected with pCGfd-GFP or -HA-BAP1 were harvested for immunoblot analysis. (C, D) Cells were scratched, visualized by a bright field microscope, and further analyzed using the Image J software. Data are presented as the mean \pm SD from three independent experiments. Statistical analysis was performed using two-way ANOVA. Significance was calculated using Tukey's HSD (** $P < 0.01$, *** $P < 0.001$). (E, F) Transwell migration or invasion assays were performed. Data are presented as the mean \pm SD from three independent experiments. Statistical analysis was performed using a Student's *t*-test (* $P < 0.05$ and ** $P < 0.01$).

the BAP1 C91S mutant did not affect wound healing, transwell migration, or invasion (Supplementary Fig. 3B-D of the SI). These results indicate that BAP1 regulates MSC migration in a deubiquitinase-dependent manner.

Regulation of MSC migration by BAP1 involves ERK signaling pathways

The signaling pathways associated with MSC migration were investigated to understand the molecular mechanisms underlying BAP1 regulation. We observed an increase in ERK1/2 phosphorylation in the BAP1-depleted MSC, whereas other signaling molecules (AKT serine 473, focal adhesion kinase tyrosine 925, p38 mitogen-activated protein kinases, and vimentin) remained unchanged (Fig. 3A). Subsequently, we examined the upstream signaling molecules involved in ERK1/2 phosphorylation. As shown in Fig. 3B, ERK1/2 phosphorylation only increased under BAP1 depletion conditions, suggesting that BAP1 directly regulates ERK1/2 phosphorylation, but not the upstream signaling molecules of ERK1/2. To identify the transcriptional targets of the ERK signaling pathway that regulate MSC migration, we examined the mRNA expression changes in several ERK target genes known to regulate MSC migration. OPN expression was increased in BAP1-depleted MSCs, but not in SNAIL or SLUG cells (Fig. 3C).

These results suggest that BAP1 expression is closely related to the regulation of MSC migration through the activation of ERK1/2 signaling.

BAP1 deubiquitinates ubiquitins on phosphorylated-ERK1/2 to suppress MSC migration

Biochemical experiments were conducted to elucidate the mechanism by which BAP1 controls ERK1/2 signaling. Immunoprecipitation revealed that transiently overexpressed FLAG-BAP1 bound to both transiently overexpressed GFP-ERK1 and GFP-ERK2 (Fig. 4A). Notably, GFP-ERK2 displayed a higher binding affinity than GFP-ERK1, suggesting that ERK2 is the preferred substrate for BAP1. We further examined the endogenous interactions between BAP1 and various signaling molecules. Surprisingly, we found that neither ERK1/2 nor any other signaling

molecules upstream of ERK bound to BAP1; only phosphorylated-ERK1/2 co-precipitated with endogenous BAP1 (Fig. 4B).

These contradictory findings prompted us to hypothesize that the co-precipitation of overexpressed GFP-ERK1 and GFP-ERK2 with BAP1 occurred because they were partially and transiently phosphorylated. To test this hypothesis, we created a GFP-ERK2 2A mutant lacking the phosphorylation sites by replacing threonine 185 and tyrosine 187 (T185 and Y187, respectively) with alanine (20, 21). GFP-ERK2 was chosen because of its greater affinity for BAP1 than GFP-ERK1. As anticipated, the GFP-ERK2 2A mutant was rarely associated with BAP1, suggesting that the phosphorylation sites (T185 and Y187) of ERK2 are essential for BAP1 binding (Fig. 4C).

Our study of the signaling pathways revealed that BAP1 depletion induced ERK1/2 phosphorylation without affecting other upstream signaling molecules (Fig. 3A, B). Collectively, these results suggest that the binding of BAP1 to phosphorylated-ERK1/2 may lead to a reduction in its phosphorylation.

Given the established role of BAP1 deubiquitinase activity in the regulation of MSC migration, we investigated whether BAP1 can alter the ubiquitination of ERK1/2. Ubiquitination of GFP-ERK2 was observed in a denaturation condition-based ubiquitination assay when expressed with HA-ubiquitin (Fig. 4D). BAP1 expression reduced the ubiquitination of GFP-ERK2, indicating that BAP1 deubiquitinates ubiquitins on GFP-ERK2 (Fig. 4D). Moreover, the proteasome inhibitor MG132 had no

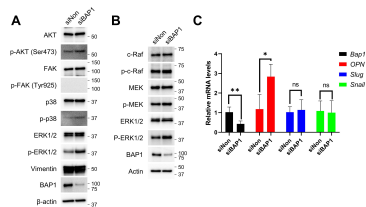


Fig. 3. BAP1 suppresses the ERK signaling pathway. (A, B) MSCs transfected with 20 nM siNon or siBAP1 were harvested for immunoblot analysis. (C) The levels of mRNA were determined using qRT-PCR. Data are presented as the mean \pm SD from three independent experiments. Statistical analysis was performed using Student's t-test (ns = non-significant, *P < 0.05 and **P < 0.01).

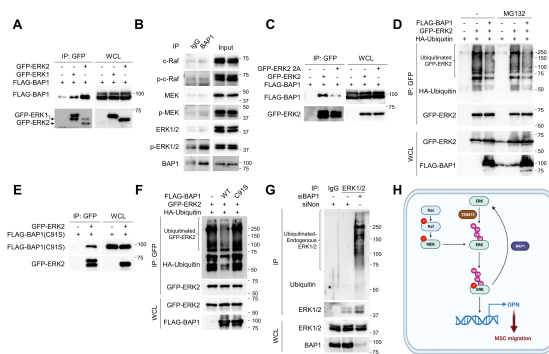


Fig. 4. BAP1 binds to ERK1/2 and regulates its ubiquitination status in a deubiquitinase activity-dependent manner. (A, C, E) 293T cells transfected with the indicated plasmids were harvested, lysed, and immunoprecipitated with an anti-GFP antibody. Thereafter, proteins were analyzed by immunoblotting using anti-FLAG and -GFP antibodies. (B) MSCs were lysed and immunoprecipitated using an anti-BAP1 antibody. Endogenous proteins were analyzed by immunoblotting using the indicated antibodies. (D, F) 293T cells transfected with the indicated plasmids were harvested, lysed under denaturing conditions, and immunoprecipitated with an anti-GFP antibody. Protein levels were analyzed by immunoblotting using anti-ubiquitin-HRP, -GFP, and -FLAG antibodies. (G) MSCs transfected with 20 nM siNon or siBAP1 were lysed under denaturing conditions and immunoprecipitated with an anti-ERK1/2 antibody. Proteins were analyzed by immunoblotting using the indicated antibodies. (H) Conceptual illustration showing the role of BAP1 in regulating MSC migration.

effect on the ubiquitination or BAP1-dependent deubiquitination of GFP-ERK2, suggesting that both processes are proteasome-independent (Fig. 4D). We examined the effect of the BAP1 C91S mutation on GFP-ERK2 ubiquitination. Although the BAP1 C91S mutant bound strongly to GFP-ERK2, it failed to deubiquitinate the ubiquitin on GFP-ERK2 (Fig. 4E, F). Finally, we studied the effect of BAP1 depletion on the ubiquitination of endogenous ERK1/2 in MSCs. The ubiquitination of endogenous ERK1/2 increased in siBAP1-transfected MSCs (Fig. 4G). These results indicate that BAP1 regulates the ERK signaling pathway via the deubiquitination of phosphorylated ERK1/2.

DISCUSSION

This study identified BAP1 as a negative regulator of MSC migration through siRNA library screening using an *in vitro* wound-healing assay. BAP1 depletion enhanced MSC migration, whereas BAP1 overexpression reduced MSC migration. Interestingly, BAP1 deubiquitinase activity, located in the UCH domain in the N-terminal region, is crucial for suppressing MSC migration. Moreover, BAP1 was found to control MSC migration through the ERK signaling pathway, with BAP1 deubiquitinating ubiquitins on phosphorylated-ERK1/2. This is the first report to demonstrate that BAP1 regulates MSC migration via the deubiquitination of ERK1/2 ubiquitins.

BAP1 deficiency is well known to induce epithelial-to-mesenchymal transition (EMT) and metastasis in numerous cancers (22-27). During EMT, cancer cells gain the ability to migrate because of the superior motility of mesenchymal cells, compared to that of epithelial cells. Additionally, BAP1 regulates EMT during trophoblast differentiation and invasion, while decreased BAP1 expression triggers EMT and enhances migration and invasion (27). In this context, we demonstrated that BAP1 depletion enhances the migratory capability of MSCs. Furthermore, the BAP1 expression pattern observed in the Human Protein Atlas supports an inverse correlation between BAP1 expression and cell motility, with blood cells, known for their high motility, showing notably lower levels of BAP1 expression (Supplementary Fig. 2 of the SI).

Our results, and those of other studies, suggest that BAP1 suppresses the migration of most cell types. However, the underlying mechanism requires further investigation. This study found that BAP1 deubiquitinase activity is required to regulate MSC migration. Many targets of BAP1 have been proposed, including histone H2AK119 and various non-histone proteins, such as IP3R3, HCF-1, KLF5, INO80, DNMT1, NCOR1, and PGC1 α (13-18). We identified a new non-histone protein target of BAP1. BAP1 depletion increased ERK1/2 phosphorylation, indicating a negative regulatory effect of BAP1 on ERK1/2 activation.

Recently, it was discovered that the K63-linked polyubiquitination of ERK1/2 is closely related to the phosphorylation status of ERK1/2 (28). TRIM15 participates in this polyubiquitination

process by increasing its interaction with MEK, an ERK1/2 upstream kinase. This interaction increases ERK1/2 phosphorylation. Our study defines BAP1 as a deubiquitinase of ERK1/2. The observed inverse relationship between BAP1 expression and ERK1/2 polyubiquitination suggests that BAP1 inhibits the ERK signaling pathway by deubiquitinating the K63-linked polyubiquitin of ERK1/2. This deubiquitination appears to reduce ERK1/2 phosphorylation by inhibiting the interaction between ERK1/2 and MEK (Fig. 4H).

A previous study identified the tumor suppressor cylindromatosis (CYLD) as a deubiquitinase that antagonizes TRIM15-mediated ERK1/2 ubiquitination (28). CYLD is a deubiquitinase that is induced and activated by nuclear factor- κ B in response to inflammatory stimuli, such as tumor necrosis factor (TNF) and interleukin-1 β . In contrast, BAP1 is a constitutively expressed deubiquitinase that regulates various cellular processes by modulating gene transcription and directly deubiquitinating target proteins (25). Moreover, BAP1 is frequently mutated or downregulated in various cancers, but not in MSCs (25). These differences may explain the divergent roles of CYLD and BAP1 in the deubiquitination of ERK1/2.

Several studies have investigated the effects of ubiquitination on the phosphorylation of target proteins (29). For example, TNF receptor-associated factor 3 is K63-linked ubiquitinated in response to viral infection, which increases its interaction with tank-binding kinase-1 and influences its phosphorylation status (30). We hypothesized that BAP1-mediated deubiquitination of ERK1/2 may cause a structural change in ERK1/2, which interferes with MEK binding and negatively regulates its phosphorylation.

Additionally, we found that OPN, a known ERK target gene, was upregulated in the BAP1-depleted MSCs. OPN plays a role in cell adhesion and migration. This implies that BAP1 influences MSC migration via ERK-mediated OPN expression.

Overall, our findings enrich the current understanding of the factors affecting MSC migration and therapeutic potency by elucidating the role and mechanisms of action of BAP1. They also suggest potential therapeutic strategies to increase the efficacy of MSCs in regenerating damaged tissues and treating various diseases by modulating BAP1 expression or deubiquitinase activity.

MATERIALS AND METHODS

Cell culture and reagents

Human MSCs (PT-2501) were obtained from Lonza (Basel, Switzerland). All the cells were cultured in complete Dulbecco's Modified Eagle's Medium (DMEM; 10-013-CVR; Corning cellgro, Manassas, VA, USA) supplemented with 10% Fetal Bovine Serum (FBS; 16000044; Thermo Fisher Scientific, Waltham, MA, USA) and 1% antibiotic-antimycotic (15240062; Thermo Fisher Scientific). The cultures were maintained at 37°C under 5% CO₂. All the cells were tested for mycoplasma using an e-mycTM plus Mycoplasma PCR detection kit (25237; Intron,

Seongnam, Gyeonggi, Korea) and maintained under mycoplasma-free conditions.

In vitro wound healing-based siRNA screening

We performed *in vitro* wound healing-based siRNA screening using the Human ON-TARGET plus siRNA Library-Deubiquitinating Enzyme (G-104705-05; Horizon Discovery, Waterbeach, UK). Approximately 2×10^5 cells were transfected with 20 nM siRNA via microporation and subsequently plated in a 12-well cell culture plate. Forty-eight hours post-transfection, a scratch was created using a pipette tip, and the culture medium was replaced with serum-free DMEM. Observations and analyses of each well were conducted using a microscope (CKX53; Olympus, Tokyo, Japan) and processed using the ImageJ software (1.52a; NIH, Bethesda, MD, USA). Human ON-TARGET plus siRNA SMART pools, siBAP1 (L-005791-00-0005; Horizon Discovery) and siNon (D-001810-10-05; Horizon Discovery), were used as controls for all the knockdown experiments.

Plasmid construction

All the ubiquitin constructs (pRK5-HA-Ubiquitin) and pcDNA3-FLAG-BAP1 were kindly provided by J. Song of Yonsei University (31). We used the pCGfd plasmid, a minimally sized CpG sequence-free plasmid that demonstrates high transfection efficiency in MSCs (19).

We have listed all the primer sequences for site-directed mutagenesis in Supplementary Table 1.

Microporation of MSCs

For the microporation of the MSCs, we followed a previously reported protocol (19). Briefly, the MSCs were trypsinized, centrifuged, and resuspended in PBS. Cell concentration was determined using a LUNA-FL™ cell counter (Logos Biosystems, Anyang, Korea). The MSCs were then transferred to 1.5 ml microcentrifuge tubes, spun down, and resuspended in a resuspension buffer (MPK1096, 10096; Thermo Fisher Scientific). We introduced 20 nM siRNA or 2 µg of plasmid into each batch of 2×10^5 cells. Using a Neon pipette and tips (MPK1096, 10096; Thermo Fisher Scientific), the resulting mixtures were microporated under pre-optimized conditions for MSCs (990 V, 40 ms, 1 pulse).

Immunoprecipitation and immunoblotting

The cells were lysed in a buffer containing 50 mM Tris-HCl (pH 7.5), 150 mM NaCl, 0.5% Triton X-100, 1 mM EDTA, and a protease inhibitor cocktail (11697498001; Roche, Penzberg, Germany) on ice for 30 min. The cell lysates were centrifuged at 13,000 rpm at 4°C for 10 min. The supernatants were transferred to a new microcentrifuge tube and incubated overnight at 4°C with 1 µg of either normal mouse IgG (sc-2025; Santa Cruz Biotechnology, Dallas, TX, USA), anti-BAP1 (sc-28383; Santa Cruz Biotechnology), or anti-GFP (sc-9996; Santa Cruz Biotechnology). Subsequently, recombinant protein G agarose (15920010; Thermo Fisher Scientific) was added to the samples,

followed by incubation for 2 h at 4°C. The samples were then centrifuged at 3,000 rpm at 4°C for 5 min and washed thrice with a lysis buffer. Samples were eluted using a sample buffer and analyzed by immunoblotting.

All the protein samples were separated using sodium dodecyl sulfate-polyacrylamide gel electrophoresis and transferred onto membranes. Protein bands were detected using a chemiluminescence imaging system (FUSION Solo X; VILBER, Collégien, France).

The primary antibodies are listed in Supplementary Table 3.

Ubiquitination assay

To assess ubiquitination under denaturing conditions, we followed the protocol described in a previous report (32). Briefly, the cells were lysed in PBS containing 1% SDS and 10 mM NEM (Sigma-Aldrich) and boiled for 10 min. We then added a lysis buffer containing 50 mM Tris-HCl (pH 7.5), 150 mM NaCl, 0.5% Triton X-100, 1 mM EDTA, protease inhibitors, and 10 mM NEM to reduce the SDS concentration to 1%. We performed immunoprecipitation using anti-GFP and ERK1/2 antibodies and analyzed ERK ubiquitination by immunoblotting.

Statistical analysis

Statistical analyses were performed using the GraphPad Prism software (version 9.5.1; La Jolla, CA, USA). In cases where only two groups were analyzed, a Student's t-test was used to determine statistical differences and significance. For the transwell migration and invasion assays, a one-way analysis of variance (ANOVA) with Tukey's honest significant difference (HSD) *post-hoc* test was used. Two-way ANOVA with Tukey's HSD *post-hoc* test was used for the *in vitro* wound healing assay. The error bars represent the standard deviation (SD).

ACKNOWLEDGEMENTS

This work was supported by grants from the National Research Foundation of Korea [NRF-2020R1C1C1006833, NRF-2022 R1A2C1011353, and CRC22011-300] and the Korea Research Institute of Bioscience and Biotechnology (KRIBB) Research Initiative Program [KGM5322321].

CONFLICTS OF INTEREST

The authors have no conflicting interests.

REFERENCES

1. Naji A, Eitoku M, Favier B, Deschaseaux F, Rouas-Freiss N and Suganuma N (2019) Biological functions of mesenchymal stem cells and clinical implications. *Cell Mol Life Sci* 76, 3323-3348
2. Nauta AJ and Fibbe WE (2007) Immunomodulatory properties of mesenchymal stromal cells. *Blood* 110, 3499-

- 3506
3. Francois M, Romieu-Mourez R, Li M and Galipeau J (2012) Human MSC suppression correlates with cytokine induction of indoleamine 2,3-dioxygenase and bystander M2 macrophage differentiation. *Mol Ther* 20, 187-195
 4. Bernardo ME and Fibbe WE (2013) Mesenchymal stromal cells: sensors and switchers of inflammation. *Cell Stem Cell* 13, 392-402
 5. Prockop DJ (2013) Concise review: two negative feedback loops place mesenchymal stem/stromal cells at the center of early regulators of inflammation. *Stem Cells* 31, 2042-2046
 6. Ankrum J and Karp JM (2010) Mesenchymal stem cell therapy: two steps forward, one step back. *Trends Mol Med* 16, 203-209
 7. Nitzsche F, Muller C, Lukomska B, Jolkkonen J, Deten A and Boltze J (2017) Concise review: MSC adhesion cascade—insights into homing and transendothelial migration. *Stem Cells* 35, 1446-1460
 8. Mun JY, Shin KK, Kwon O, Lim YT and Oh DB (2016) Minicircle microporation-based non-viral gene delivery improved the targeting of mesenchymal stem cells to an injury site. *Biomaterials* 101, 310-320
 9. Fu X, Liu G, Halim A, Ju Y, Luo Q and Song AG (2019) Mesenchymal stem cell migration and tissue repair. *Cells* 8, 784
 10. Swatek KN and Komander D (2016) Ubiquitin modifications. *Cell Res* 26, 399-422
 11. Mevissen TET and Komander D (2017) Mechanisms of deubiquitinase specificity and regulation. *Annu Rev Biochem* 86, 159-192
 12. Masclef L, Ahmed O, Estavoyer B et al (2021) Roles and mechanisms of BAP1 deubiquitinase in tumor suppression. *Cell Death Differ* 28, 606-625
 13. Machida YJ, Machida Y, Vashisht AA, Wohlschlegel JA and Dutta A (2009) The deubiquitinating enzyme BAP1 regulates cell growth via interaction with HCF-1. *J Biol Chem* 284, 34179-34188
 14. Ruan HB, Han X, Li MD et al (2012) O-GlcNAc transferase/host cell factor C1 complex regulates gluconeogenesis by modulating PGC-1 α stability. *Cell Metab* 16, 226-237
 15. Qin J, Zhou Z, Chen W et al (2015) BAP1 promotes breast cancer cell proliferation and metastasis by deubiquitinating KLF5. *Nat Commun* 6, 8471
 16. Bononi A, Giorgi C, Patergnani S et al (2017) BAP1 regulates IP3R3-mediated Ca²⁺ flux to mitochondria suppressing cell transformation. *Nature* 546, 549-553
 17. Yu L, Jearawiriyapaisarn N, Lee MP et al (2018) BAP1 regulation of the key adaptor protein NCoR1 is critical for gamma-globin gene repression. *Genes Dev* 32, 1537-1549
 18. Lee HS, Seo HR, Lee SA, Choi S, Kang D and Kwon J (2019) BAP1 promotes stalled fork restart and cell survival via INO80 in response to replication stress. *Biochem J* 476, 3053-3066
 19. Cha EB, Shin KK, Seo J and Oh DB (2020) Antibody-secreting macrophages generated using CpG-free plasmid eliminate tumor cells through antibody-dependent cellular phagocytosis. *BMB Rep* 53, 442-447
 20. Payne DM, Rossomando AJ, Martino P et al (1991) Identification of the regulatory phosphorylation sites in pp42/mitogen-activated protein kinase (MAP kinase). *EMBO J* 10, 885-892
 21. Haystead TA, Dent P, Wu J, Haystead CM and Sturgill TW (1992) Ordered phosphorylation of p42mapk by MAP kinase kinase. *FEBS Lett* 306, 17-22
 22. Park CM, Lee JE and Kim JH (2020) BAP1 functions as a tumor promoter in prostate cancer cells through EMT regulation. *Genet Mol Biol* 43, e20190328
 23. Hu D, Zheng Y, Ou X, Zhang L, Du X and Shi S (2022) Integrated analysis of anti-tumor roles of BAP1 in osteosarcoma. *Front Oncol* 12, 973914
 24. Shen C, Wang Y, Wei P and Du X (2016) BRCA1-associated protein 1 deficiency in lung adenocarcinoma predicts poor outcome and increased tumor invasion. *BMC Cancer* 16, 670
 25. Kwon J, Lee D and Lee SA (2023) BAP1 as a guardian of genome stability: implications in human cancer. *Exp Mol Med* 55, 745-754
 26. Perkill S, Andricovich J, Kai Y and Tzatsos A (2020) BAP1 is a haploinsufficient tumor suppressor linking chronic pancreatitis to pancreatic cancer in mice. *Nat Commun* 11, 3018
 27. Perez-Garcia V, Lea G, Lopez-Jimenez P et al (2021) BAP1/ASXL complex modulation regulates epithelial-mesenchymal transition during trophoblast differentiation and invasion. *Elife* 10, e63254
 28. Zhu G, Herlyn M and Yang X (2021) TRIM15 and CYLD regulate ERK activation via lysine-63-linked polyubiquitination. *Nat Cell Biol* 23, 978-991
 29. Barbour H, Nkwe NS, Estavoyer B et al (2023) An inventory of crosstalk between ubiquitination and other post-translational modifications in orchestrating cellular processes. *iScience* 26, 106276
 30. Zhou Y, He C, Yan D et al (2016) The kinase CK1 α controls the antiviral immune response by phosphorylating the signaling adaptor TRAF3. *Nat Immunol* 17, 397-405
 31. Seo J, Lee EW, Shin J et al (2018) K6 linked polyubiquitylation of FADD by CHIP prevents death inducing signaling complex formation suppressing cell death. *Oncogene* 37, 4994-5006
 32. Seo J, Lee EW, Sung H et al (2016) CHIP controls necroptosis through ubiquitylation- and lysosome-dependent degradation of RIPK3. *Nat Cell Biol* 18, 291-302